



## Optoelectronic and electrochemical properties of nickel oxide (NiO) films deposited by DC reactive magnetron sputtering

B. Subramanian<sup>a</sup>, M. Mohamed Ibrahim<sup>b</sup>, V. Senthilkumar<sup>c</sup>, K.R. Murali<sup>a</sup>, VS. Vidhya<sup>a</sup>, C. Sanjeeviraja<sup>c</sup>, M. Jayachandran<sup>a,\*</sup>

<sup>a</sup> Electrochemical Materials Science Division, Central Electrochemical Research Institute, Karaikudi 630 006, India

<sup>b</sup> Birla Institute of Technology and Science, Pilani, Dubai, UAE

<sup>c</sup> School of Physics, Alagappa University, Karaikudi 630 003, India

### ARTICLE INFO

#### Article history:

Received 2 June 2008

Received in revised form

14 August 2008

Accepted 21 August 2008

#### Keywords:

Nickel oxide

Thin films

Semiconductor

Electrochromism

DC magnetron sputtering

### ABSTRACT

Nickel oxide (NiO) thin films were deposited onto glass substrates by the DC reactive magnetron sputtering technique. The as-deposited films were post-annealed in air at 450–500 °C for 5 h. The effect of annealing on the structural, microstructural, electrical and optical properties were studied by X-ray diffraction (XRD), atomic force microscope (AFM), four-probe resistivity measurement and UV-vis spectrophotometer. XRD studies indicated cubic structure with a lattice parameter of 0.4193 nm. The band gap of the films was found to be 3.58 eV. Fourier transform infrared (FTIR) studies indicated a broad spectrum centered at 451.6 cm<sup>-1</sup>. Photoluminescence studies exhibited room temperature emission at 440 nm. Cyclic voltammetry studies in 1 M KOH solution revealed the electrochromic nature of the NiO films prepared in the present study.

© 2008 Elsevier B.V. All rights reserved.

### 1. Introduction

A number of nickel oxides with various oxidation states of nickel such as nickelous oxide (NiO), nickel dioxide (NiO<sub>2</sub>), nickel sesquioxide (Ni<sub>2</sub>O<sub>3</sub>), nickelosic oxide (Ni<sub>3</sub>O<sub>4</sub>) and nickel peroxide (NiO<sub>4</sub>) have been reported. Amongst these, NiO has rhombohedral or cubic structure and possesses pale green color. The stoichiometry of NiO is roughly indicated by the color of the sample [1]. The color of NiO is highly sensitive to the presence of higher valence states of nickel even in traces. It exhibits widely varying magnetic, optical, electronic and electrochemical properties depending on the synthesis process and the resulting defect structures. The presence of nickel cation vacancy and/or interstitial oxygen in NiO crystalline lattice results in non-stoichiometric NiO<sub>x</sub>.

Interest in nickel oxide thin films has been growing fast due to their importance in many applications in science and technology. It is an attractive material for use as an antiferromagnetic layer [2], p-type transparent conducting film [3], as an active electrode in electrochromic devices [4] and functional sensing layer for developing chemical sensors [5]. NiO exhibits p-type

semiconducting nature with wide band gap energy in the range of 3.5–4.0 eV [6].

Appreciable conductivity can also be achieved in NiO film by creating Ni vacancies or substituting Li for Ni at Ni sites [7]. Most attractive features of NiO are: (i) excellent durability and electrochemical stability, (ii) low materials cost, (iii) promising ion storage material in terms of cyclic stability, (iv) large spin optical density and (v) possibility of manufacturing by variety of techniques.

NiO has been investigated as a promising electrochromic layer for smart window applications. The electrochromic effect in these materials is related to a reversible coloration/bleaching process by means of a simultaneous injection/extraction of both ions and electrons due to applied voltage. Electrochromism in NiO is complicated although it is generally accepted that the transition from a colored to a bleached state is related to a charge transfer process between Ni<sup>2+</sup> and Ni<sup>3+</sup> ions [8]. Several techniques like spray pyrolysis [9], sputtering [10], vacuum evaporation [3], electron beam evaporation [11], chemical deposition [12], sol-gel [13], pulse laser deposition [14] and plasma-enhanced chemical vapor deposition [15] have been employed for the deposition of NiO thin films. It is well known that the structural properties and surface morphology of materials in thin-film form depend on the deposition conditions and post-deposition annealing. In this work, the DC reactive magnetron sputtering technique was used to

\* Corresponding author. Tel.: +91 4565 227550; fax: +91 4565 227713.

E-mail address: [jayam54@yahoo.com](mailto:jayam54@yahoo.com) (M. Jayachandran).

deposit NiO films. The structural, morphological, electrical, optical and electrochromic properties of these films were studied and presented in detail.

## 2. Experimental techniques

Thin NiO films were deposited on glass substrates using a Hind Hivac Magnetron Sputtering system. The films were deposited by DC reactive magnetron sputtering from a Ni target (50 mm in diameter, 3 mm in thickness, 99.9% pure) in a mixture of oxygen and argon onto glass substrates. The relative partial pressure of oxygen to argon, defined as the ratio of  $p(O_2)/p(O_2+Ar)$ , was fixed at 33.3%. A sputtering power of 150 W was used. Sputtering deposition was performed at a gas pressure of  $5 \times 10^{-3}$  mbar. Prior to deposition, the glass substrates were boiled in chromic acid, followed by washing in deionized water. The substrates were then cleaned with acetone using an ultrasonic cleaner. The deposition time was 10 min. Thickness of the films, measured by gravimetry, was 0.32  $\mu\text{m}$ . The films were characterized by X-ray diffraction (XRD) studies using an X'pert Pro PANalytical X-ray diffractometer. Optical absorption spectra were studied using a U 3400 UV-vis-NIR spectrophotometer. Fourier transform infrared (FTIR) studies were made with Perkin Elmer system. Electrical conductivity measurements were made by the four-probe technique. Surface morphology was studied with molecular imaging atomic force microscope (AFM) system. Chemical binding energy analysis was carried out using a Multilab 2000 X-ray photoelectron spectroscope with Mg K $\alpha$  (1253.6 eV) X-ray source operating at 10 kV and 10 mA. Electrochemical studies were made using a PARSTAT 2273 Advanced Electrochemical System. Cary Ellipse Fluorescence Spectrophotometer (VARIAN) was used to record the photoluminescence spectra employing PBS photo detector and 150 Xe arc discharge lamp as the excitation source.

## 3. Results and discussion

XRD pattern of the NiO thin films, prepared by the DC reactive magnetron sputtering process, is shown in Fig. 1a. A broad peak is observed at 25° in the XRD pattern, indicating the poor crystallinity of the films. To improve the crystallinity, the films were annealed in air at different temperatures in the range of 400–500 °C. The diffraction pattern of the film annealed at 400 °C shows the presence of weak diffraction peaks from (111) and (200) lattice planes (Fig. 1b). As the annealing temperature was increased to 500 °C, the NiO films showed brown color and the XRD pattern exhibited intense peaks corresponding to the (111) and (200) orientations of cubic NiO (JCPDS File no. 89-7130) as shown in Fig. 1c. An additional plane (220), along with (111) and (200) planes, is also observed in this case. The structural parameters, like, grain size, lattice parameter, strain and dislocation density were calculated and are presented in Tables 1 and 2 for the films annealed at 400 and 500 °C, respectively. The calculated lattice parameter values of 0.4190–0.4193 nm agree well with the standard value (0.4195 nm) for FCC NiO phase [3]. The grain size is found to increase with the increase in annealing temperature. The strain and dislocation density values are found to decrease with increase in annealing temperature.

AFM was used to evaluate the surface topography of the DC reactive magnetron sputtered NiO thin films. The topographical 3D and 2D micrographs recorded over an area of  $2 \mu\text{m} \times 2 \mu\text{m}$  of the as-deposited and annealed NiO thin films are shown in Figs. 2a–b and 3a–b, respectively. The 3D micrographs show the presence of hills on the top of the surface. The sharpness of the hills and also the number of hills are found to decrease for

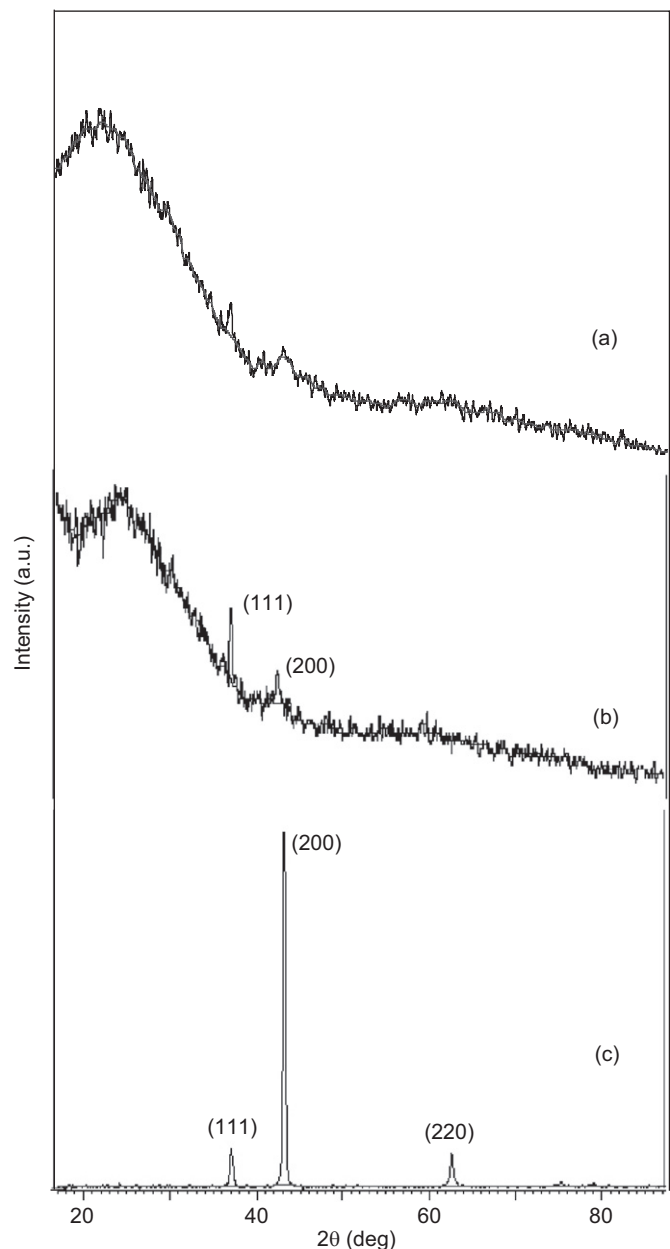


**Fig. 1.** XRD pattern of NiO films deposited by DC reactive magnetron sputtering: (a) as-deposited, (b) annealed at 400 °C and (c) annealed at 500 °C.

the NiO thin films annealed at 500 °C. The roughness profile also confirms that the increase in annealing temperature from 400 to 500 °C results in decreased roughness from 22 to 11 nm, respectively.

The absorbance spectrum of the NiO film annealed at 500 °C was recorded in the wavelength range 300–1000 nm, the sharp decrease in the absorption spectrum at 310 nm may be attributed to the band gap absorption of NiO and then stabilizes (Fig. 4). The band gap of the film was estimated from the following equation:

$$\alpha = A(hv - E_g)^n$$

where  $\alpha$  is the absorption coefficient and  $E_g$  is the band gap of the material. For direct band-to-band allowed transition, the value of

**Table 1**

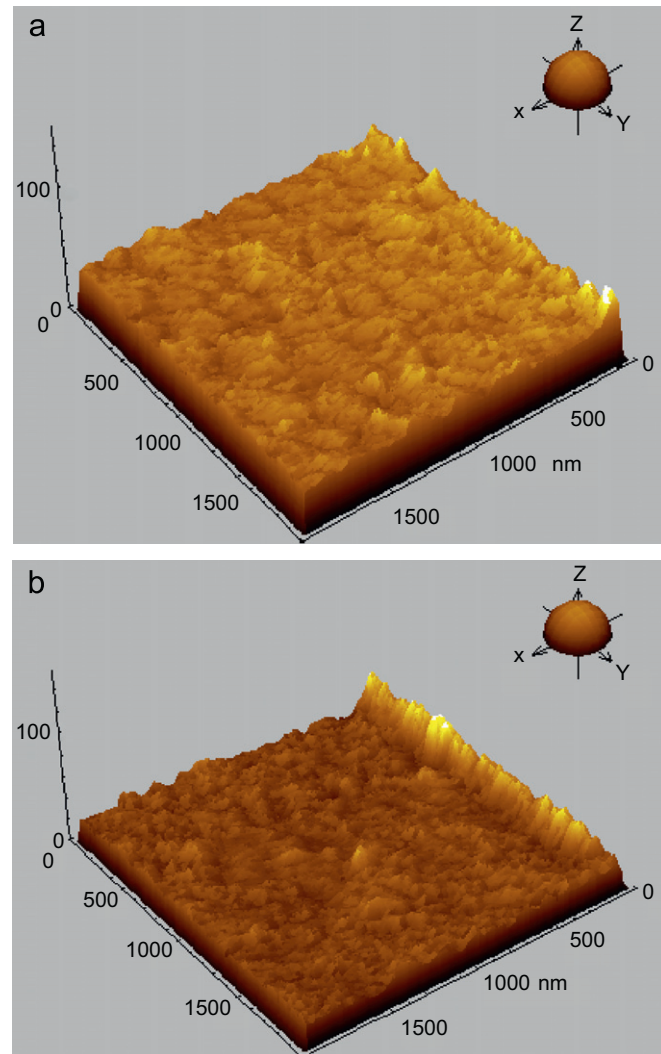
Structural parameters of as-deposited DC magnetron sputtered NiO Film

Lattice parameter a (nm)	d-spacing calculated (nm)	d-spacing standard (nm)	d(hkl)	Grain size D (nm)	Strain $\varepsilon \times 10^{-3}$ (line $^{-2}$ m $^{-4}$ )	Dislocation density $\delta \times 10^{16}$ (line m $^{-1}$ )
0.4193	0.2409	0.2421	(111)	15.98	9.69	2.20
	0.2084	0.2097	(200)	9.12	2.74	1.08

**Table 2**

Structural parameters of DC magnetron sputtered NiO film annealed at 500 °C

Lattice parameter a (nm)	d-spacing calculated (nm)	d-spacing standard (nm)	d(hkl)	Grain size D (nm)	Strain $\varepsilon \times 10^{-3}$ (line $^{-2}$ m $^{-4}$ )	Dislocation density $\delta \times 10^{16}$ (line m $^{-1}$ )
0.4190	0.2425	0.2422	(111)	26.26	1.11	1.52
	0.2095	0.2097	(200)	28.09	0.88	1.12
	0.1485	0.1489	(220)	29.03	0.61	0.75

**Fig. 2.** Three-dimensional micrographs of the NiO films: (a) as-deposited and (b) post-annealed at 500 °C.

$n$  is taken as  $\frac{1}{2}$ . Accordingly, the results obtained from the absorption data were drawn as a plot of  $(\alpha h\nu)^2$  vs. photon energy ( $h\nu$ ) to find the value of  $E_g$  (Fig. 5). It is observed from Fig. 5 that

there exists a linear dependence of  $(\alpha h\nu)^2$  with  $(h\nu)$  in the high photon energy region, while some exponential variation is found in the low photon energies. Extrapolation of the linear portion to the  $h\nu$  axis yielded a band gap value of 3.58 eV, which is in good agreement with the reported band gap values of 3.15–3.80 eV for NiO films [16,17].

Photoluminescence studies indicated that for an excitation of 440 nm, a broad emission peak is observed at 595.07 nm (Fig. 6) for the sputtered NiO thin film, which is in the visible region showing the good optical quality of the film.

The hot probe technique was used to find the nature of the as-deposited as well as heat-treated NiO films. The experiment was carried out by contacting the NiO film with hot probe at one end and cold probe at the other, which were connected to the positive and negative terminals of a nA current meter, respectively. When hot probe momentarily touched the film, a positive current was observed, which showed the nature of the NiO films to be p-type. Resistivity of the films was measured by the four-probe method using the relation

$$\rho = 4.532 \times (V/I) \times t$$

where  $\rho$  is the resistivity,  $V$  is the applied voltage and  $I$  is the current and  $t$  is the thickness. The value of resistivity is  $1.79 \times 10^{-4} \Omega \text{cm}$ . The conduction mechanism of the NiO film is related to the vacancies existing in the structure. The electrical properties of NiO films are associated with their microstructure and composition, and consequently on the deposition environment [18–21]. Non-stoichiometric  $\text{NiO}_x$  also is known as a p-type semiconductor [17]. The defects that are the cause for hole conductivity are  $\text{Ni}^{2+}$  ion vacancies. Each vacancy is replaced by two  $\text{Ni}^{3+}$  ions, which act as electron acceptors. However, crystalline NiO film with (200) orientation is formed with near-stoichiometric ratio. Pure stoichiometric NiO is an insulator with high resistivity ( $\rho > 10^{13} \Omega \text{cm}$ ) at room temperature. In this study, the NiO films were oriented in both (111) and (200) directions. The value of resistivity obtained in this work is much lower than the values reported earlier [22]. The lower resistivity values obtained in this work may be due to the fact that post-annealing of the films brought about non-stoichiometric  $\text{NiO}_x$ . To confirm this, elemental compositional analysis of Ni and O was carried out by X-ray photoelectron spectroscopy (XPS) studies. Fig. 7 shows the XPS survey spectrum and the presence of Ni 2p and O 1s peaks for the NiO film annealed at 500 °C. The atomic percentage of Ni and O was calculated as 47.6% and 51.3%, which

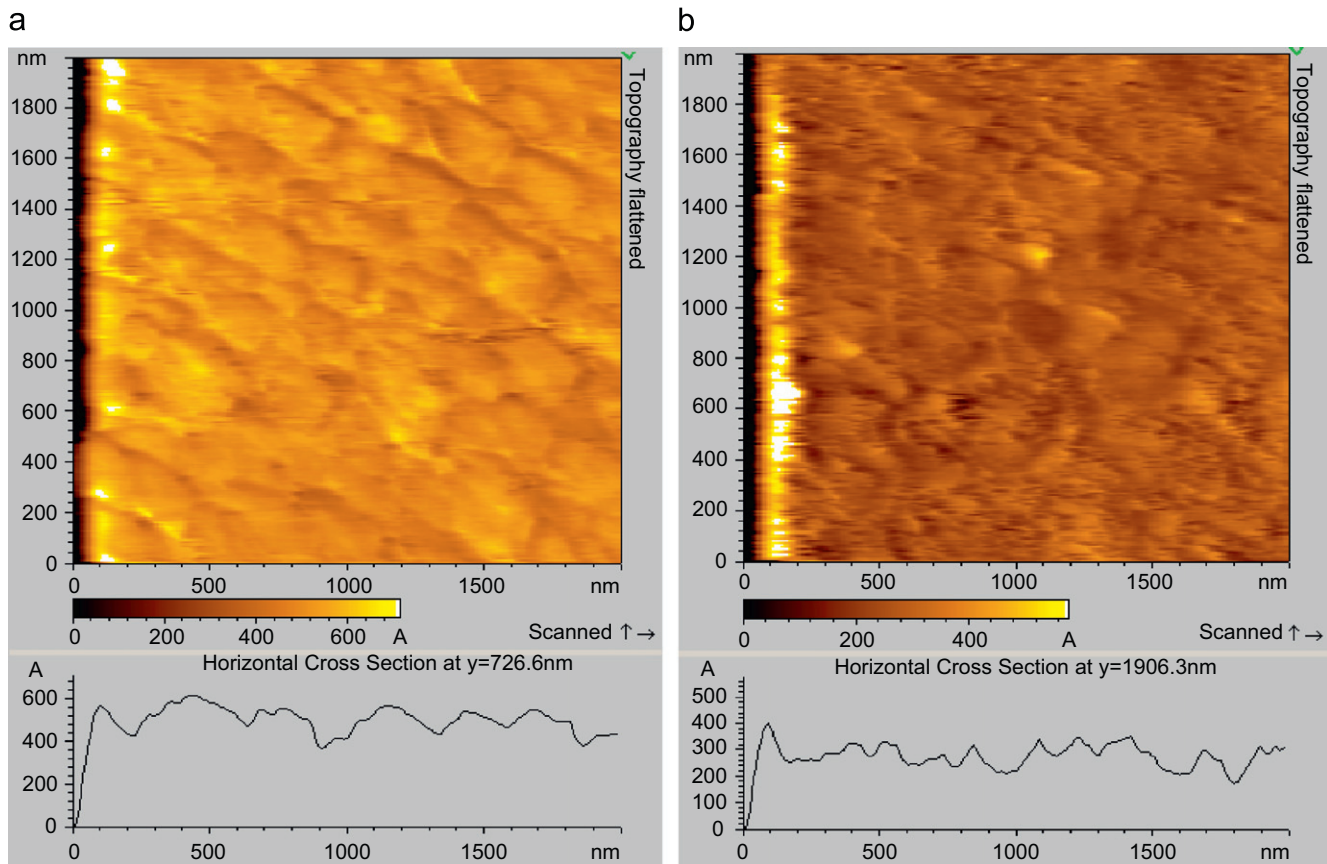


**Fig. 3.** Two-dimensional micrographs and line profiles of the (a) as-deposited and (b) post-annealed at 500 °C films.

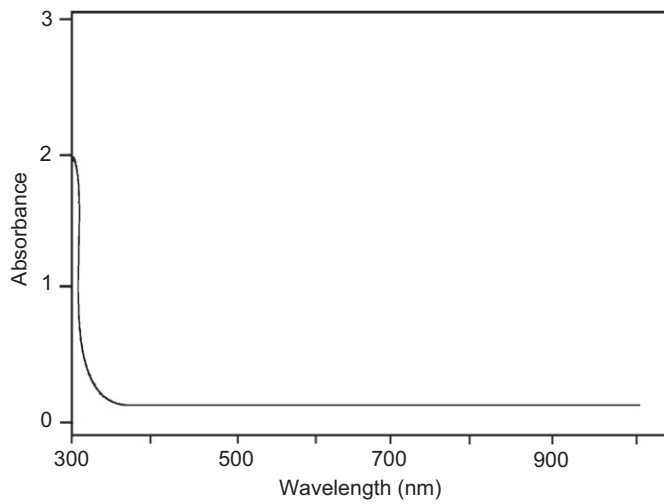


**Fig. 4.** Absorbance spectrum of NiO film.

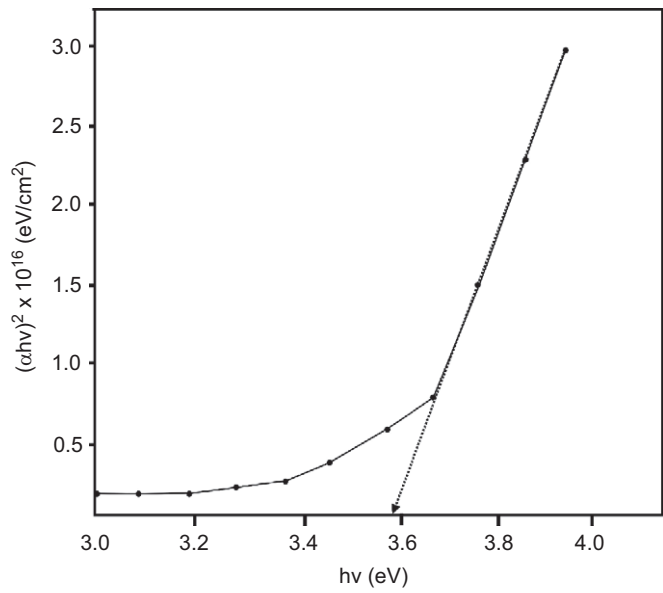


**Fig. 5.** Plot of  $(\alpha h\nu)^2$  vs.  $h\nu$  for NiO film annealed at 500 °C.

reveals the presence of oxygen in excess of Ni. It shows that the film is non-stoichiometric NiO, i.e.  $\text{NiO}_x$  that confirms the formation of  $\text{Ni}^{2+}$  vacancies to impart p-type conductivity to these annealed films [7,9].

Fig. 8 shows the FTIR transmission spectra of the NiO film, which exhibits a broad peak in the range of 450–470 cm<sup>-1</sup>. The

peak attains maximum at 451.6 cm<sup>-1</sup>. This is due to the stretching vibration of the Ni–O bond of nickel oxide [23].

Cyclic voltammograms (CVs) performed in 1 M KOH at a fixed scan rate of 50 mV s<sup>-1</sup>, revealed electrochromic behavior of NiO

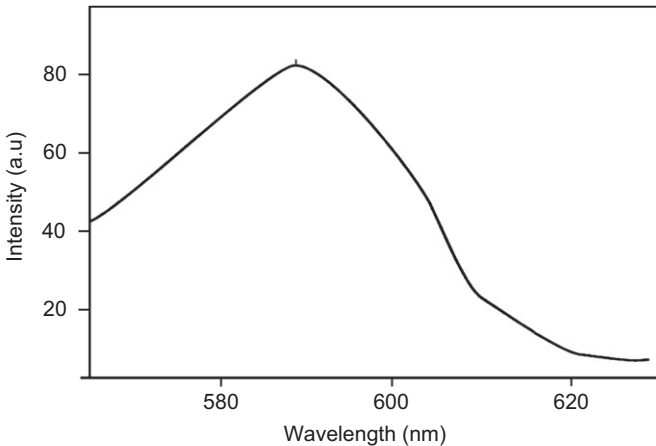


**Fig. 6.** Photoluminescence spectrum of NiO film post-annealed at 500 °C.

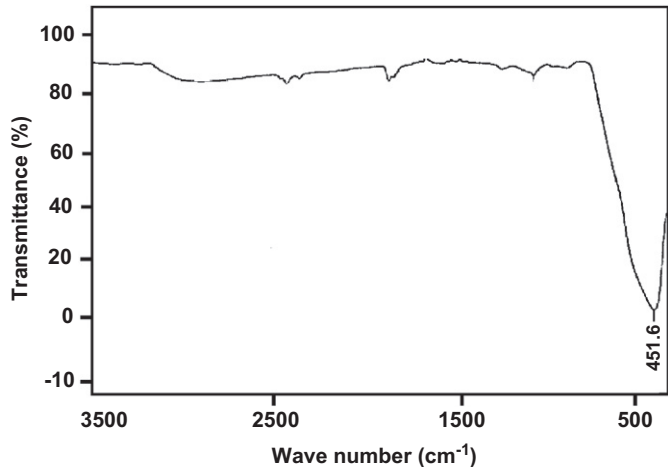


**Fig. 8.** FTIR spectrum of NiO film post-annealed at 500 °C.

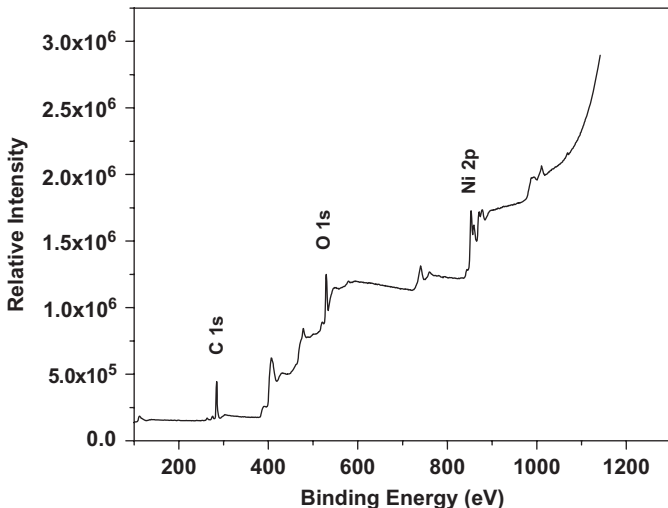
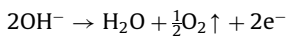
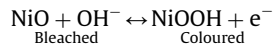


**Fig. 7.** XPS survey spectrum of NiO film post-annealed at 500 °C.

thin films in the voltage range from –0.3 to 0.9 V. Fig. 9a shows the CV of NiO, for 100 cycles, where a well-resolved anodic peak ( $\text{Ni}^{2+} \rightarrow \text{Ni}^{3+} + \text{e}^-$ ) is observed at 364.3 mV ( $E_a$ ). At this peak, the color of the NiO is changed from transparent to deep brown color. Cathodic peak ( $\text{Ni}^{3+} + \text{e}^- \rightarrow \text{Ni}^{2+}$ ) is observed at 156.9 mV ( $E_c$ ) and at this peak, the color is again changed to transparent from brown color. Fig. 9b–e shows the voltammograms for different cycles and Table 3 shows the peak potential values ( $E_a$  and  $E_c$ ) and the corresponding current density values for the cathodic ( $I_a$ ) and anodic ( $I_c$ ) peaks. From Fig. 9a–e, it is clearly observed that, as the number of cycle increases, the anodic and cathodic peaks in the voltammograms are shifted anodically towards right side as shown in Table 3. This is due to the degradation (increase in porosity) of the working electrode (NiO). During the anodic potential scan, i.e. from –0.3 to 0.9 V, current remains almost zero up to 350 mV and later it increases sharply due to the process of oxidation of  $\text{Ni}^{2+}$  to  $\text{Ni}^{3+}$  causing a deep brown coloration of the film. The strong increase in current at the end of anodic sweep is associated with the oxygen evolution reaction according to the following equation:



During the cathodic scan, i.e. from 0.9 to –0.3 V, one cathodic peak is observed at 156.9 mV (SCE) at which bleaching of the colored NiO film happens. Coloration and bleaching of NiO film is associated with the insertion and deinsertion of  $\text{OH}^-$  ions and electrons in the film. In this way, all NiO samples exhibit anodic coloration and cathodic bleaching according to the following reaction:



Here, it is interesting to note that without affecting the metal–oxygen bond, coloration or bleaching in nickel oxide occurs by the extraction/insertion of 3d electrons [24]. The top of the valence band of nickel oxide consists of nickel 3d states [25] in contrast to the oxygen 2p states for most other oxides. Therefore, there are no fundamental requirements for nickel oxide films to be hydrogen containing in order to possess electrochromic properties. Partially filled valence band or, in other words, electron vacancies on nickel atoms correspond to the colored states and in the bleached state, the valence band is full. This type of coloration mechanism is consistent with the p-type conductivity reported for NiO films containing excess oxygen [26]. The oxidation peak prior to current increase due to oxygen evolution is associated with the deep brown coloration of the film, whereas the bleaching process is associated with the reduction peak, in agreement with the anodic electrochromic nature of nickel oxide [27].

#### 4. Conclusions

NiO films were successfully deposited by the DC reactive magnetron sputtering technique. The weakly crystalline nature of the NiO film was changed to strongly crystalline nature with FCC structure, after annealing the films at 500 °C. Uniform surface coverage with fine-grained structure was observed from AFM analysis. p-Type films with low resistivity of  $1.79 \times 10^{-4} \Omega \text{ cm}$  were obtained. Photoluminescence studies confirmed the good optical quality of the NiO films. The FTIR transmittance spectra showed a broad absorption maximum centered at  $451.6 \text{ cm}^{-1}$ . The color change of the NiO film, from transparent to dark brown, was observed by cyclic voltammetry.

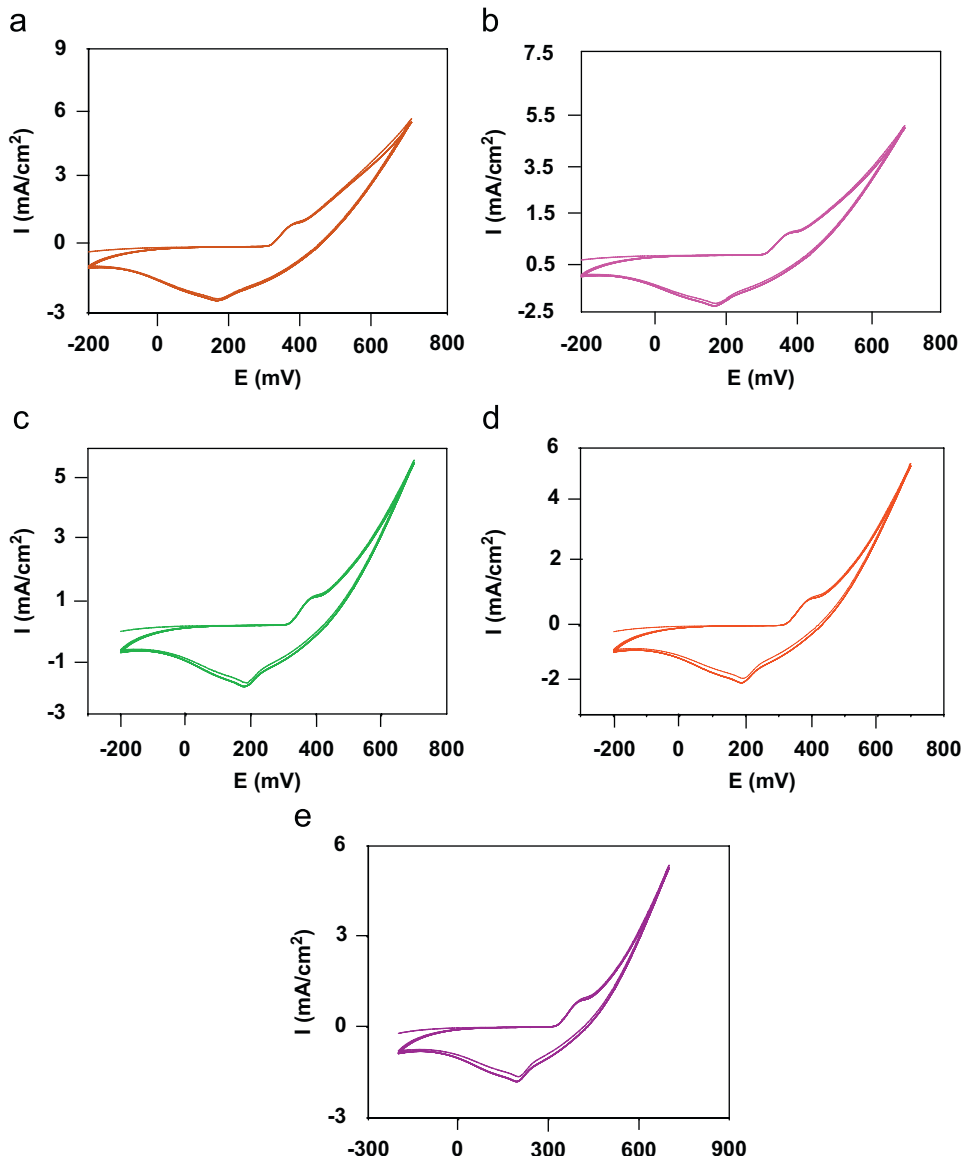


**Fig. 9.** CVs of NiO films for different cycles: (a) 100 cycles, (b) 200 cycles, (c) 300 cycles, (d) 400 cycles and (e) 500 cycles.

**Table 3**  
Potential and current values for anodic and cathodic peaks of NiO films

Number of cycles	$E_c$ (mV)	$E_a$ (mV)	$I_c$ ( $\text{mA cm}^{-2}$ )	$I_a$ ( $\text{mA cm}^{-2}$ )
100	156.9	364.3	-2.47	0.98
200	172.1	375.0	-2.28	0.94
300	178.2	379.5	-2.08	0.90
400	192.0	388.7	-1.90	0.88
500	199.6	393.3	-1.82	0.81

## References

- [1] A. Berry, Kunz, J. Phys. C: Solid State Phys. 14 (1981) L455.
- [2] S.R. Krishnakumar, M. Liberati, C. Grazioli, M. Veronese, S. Turchini, P. Luches, S. Valeri, C. Carbone, J. Magn. Magn. Mater. 310 (2007) 203.
- [3] B. Sasi, K.G. Gopchandran, P.K. Manoj, P. Koshy, P. Prabhakara Rao, V.K. Vaidyan, Vacuum 68 (2002) 211.
- [4] H.Y. Ryu, G.P. Choi, W.S. Lee, J.S. Park, J. Mater. Sci. Lett. 39 (2004) 4375.
- [5] S.A. Mohammed, A.A. Atel, H. kamal, K. Abdal- Hady, Physica B 311 (2002) 366.
- [6] J. Arakaki, R. Reyes, M. Horn, W. Estada, Sol. Energy Mater. Sol. Cells 37 (1995) 33.
- [7] P.S. Patil, L.D. Kadam, Appl. Surf. Sci. 199 (2002) 211.
- [8] C.G. Granquist, Handbook of Inorganic Electrochromic Materials, Elsevier, Amsterdam, 1995.
- [9] J.D. Desai, Sun Ki. Min, Kwang-Deog Jung, Oh-Shim Joo, Appl. Surf. Sci. 253 (2006) 1781.
- [10] H.Y. Ryu, G.P. Choi, W.S. Lee, J.S. Park, J. Mater. Sci. Lett. 39 (2004) 4375.
- [11] A. Agarwal, H.R. Habibi, R.K. Agarwal, J.P. Cronin, D.M. Roberts, C.P.R. Sue, C.M. Lampert, Thin Solid Films 221 (1992) 239.
- [12] M.A. Vidales-Hurtado, A. Mendoza-Galvan, Mater. Chem. Phys. 107 (2008) 33.
- [13] R.C. Korosec, P. Bukovec, Acta Chim. Slo. 53 (2006) 136.
- [14] M. Tanaka, M. Mukai, Y. Fujimori, M. Kondoh, Y. Tasaka, H. Baba, S. Usami, Thin solid films 281–282 (1996) 453.
- [15] E. Fujii, A. Tomozawa, S. Fujii, H. Torii, M. Hattori, R. Takayama, Jpn. J. Appl. Phys. 32 (1993) L1448.
- [16] H. Sato, T. Minami, S. Takata, T. Yamada, Thin Solid Films 236 (1993) 27.
- [17] P. Puspharajah, S. Radhakrishna, A.K. Aroif, J. Mater. Sci. 32 (1997) 3001.
- [18] O. Kohimoto, H. Nakagawa, F. Ono, A. Chayahara, J. Magn. Magn. Mater. 226–230 (2001) 1627.

- [19] Y.M. Lu, W.S. Hwang, J.S. Yang, *Surf. Coat. Technol.* 155 (2002) 231.
- [20] H.L. Chen, Y.M. Lu, W.S. Hwang, *Surf. Coat. Technol.* 198 (2005) 138.
- [21] H.L. Chen, Y.M. Lu, W.S. Hwang, *Thin Solid Films* 514 (2006) 361.
- [22] H.L. Chen, Y. Sheng Yang, *Thin Solid Films* 516 (2008) 5590.
- [23] R. Cerc Korosec, P. Bukovec, B. Pilhar, A. Surca Vuk, B. Orel, G. Drazic, *Solid State Ionics* 165 (2003) 191.
- [24] A. Azena, L. Kullman, G. Vaivars, H. Nardberg, C.G. Granquist, *Solid State Ionics* 113 (1988) 449.
- [25] J. Hugal, M. Kamal, *J. Phys. Condens. Matter* 9 (1997) 647.
- [26] E. Iguchi, K. Akashi, *J. Phys. Soc. Jpn.* 61 (1992) 3385.
- [27] J.I. Garcia-Miquel, Q. Zhang, S.J. Allen, A. Rougier, A. Blyc, H.O. Davies, A.C. Jones, T.J. Leedham, P. Williams, S.A. Impey, *Thin Solid Films* 434 (2003) 165.